

Video Article

# Visualization of Bacterial Toxin Induced Responses Using Live Cell Fluorescence Microscopy

Peter A. Keyel<sup>1</sup>, Michelle E. Heid<sup>1</sup>, Simon C. Watkins<sup>2</sup>, Russell D. Salter<sup>1</sup>

<sup>1</sup>Department of Immunology, University of Pittsburgh School of Medicine

<sup>2</sup>Department of Cell Biology and Physiology, University of Pittsburgh School of Medicine

Correspondence to: Russell D. Salter at [rds@pitt.edu](mailto:rds@pitt.edu)

URL: <https://www.jove.com/video/4227>

DOI: [doi:10.3791/4227](https://doi.org/10.3791/4227)

Keywords: Immunology, Issue 68, Cellular Biology, Physiology, streptolysin O, pore-forming toxin, cholesterol-dependent cytolysin, live cell imaging, fluorescence microscopy

Date Published: 10/1/2012

Citation: Keyel, P.A., Heid, M.E., Watkins, S.C., Salter, R.D. Visualization of Bacterial Toxin Induced Responses Using Live Cell Fluorescence Microscopy. *J. Vis. Exp.* (68), e4227, doi:10.3791/4227 (2012).

## Abstract

Bacterial toxins bind to cholesterol in membranes, forming pores that allow for leakage of cellular contents and influx of materials from the external environment. The cell can either recover from this insult, which requires active membrane repair processes, or else die depending on the amount of toxin exposure and cell type<sup>1</sup>. In addition, these toxins induce strong inflammatory responses in infected hosts through activation of immune cells, including macrophages, which produce an array of pro-inflammatory cytokines<sup>2</sup>. Many Gram positive bacteria produce cholesterol binding toxins which have been shown to contribute to their virulence through largely uncharacterized mechanisms.

Morphologic changes in the plasma membrane of cells exposed to these toxins include their sequestration into cholesterol-enriched surface protrusions, which can be shed into the extracellular space, suggesting an intrinsic cellular defense mechanism<sup>3,4</sup>. This process occurs on all cells in the absence of metabolic activity, and can be visualized using EM after chemical fixation<sup>4</sup>. In immune cells such as macrophages that mediate inflammation in response to toxin exposure, induced membrane vesicles are suggested to contain cytokines of the IL-1 family and may be responsible both for shedding toxin and disseminating these pro-inflammatory cytokines<sup>5,6,7</sup>. A link between IL-1 $\beta$  release and a specific type of cell death, termed pyroptosis has been suggested, as both are caspase-1 dependent processes<sup>8</sup>. To sort out the complexities of this macrophage response, which includes toxin binding, shedding of membrane vesicles, cytokine release, and potentially cell death, we have developed labeling techniques and fluorescence microscopy methods that allow for real time visualization of toxin-cell interactions, including measurements of dysfunction and death (**Figure 1**). Use of live cell imaging is necessary due to limitations in other techniques. Biochemical approaches cannot resolve effects occurring in individual cells, while flow cytometry does not offer high resolution, real-time visualization of individual cells. The methods described here can be applied to kinetic analysis of responses induced by other stimuli involving complex phenotypic changes in cells.

## Video Link

The video component of this article can be found at <https://www.jove.com/video/4227/>

## Protocol

### 1. Purification of Streptolysin O (SLO)

1. Inoculate 20 ml overnight culture of BL21 GOLD cells containing pBADgIII-SLOhis plasmid<sup>9</sup> into 0.5 L LB broth and add 500  $\mu$ l 50 mg/ml ampicillin. Shake culture at 225 rpm at 37 °C until OD<sub>600</sub> = 0.6, usually ~1.5 hr. Centrifuge 1 ml bacteria (considered T<sub>0</sub>) at 10,000 x g 5 min, dissolve pellet in 140  $\mu$ l 1x SDS sample buffer/1 OD and sonicate to shear DNA for protein purity analysis.
2. Induce bacteria with the addition of 5 ml 20% arabinose to culture, shake at 225 rpm at room temp for 3 hr. Collect 1 ml of bacteria, centrifuge and dissolve in 1x SDS sample buffer as above for T<sub>3</sub> time point for purity analysis.
3. Collect remaining bacteria in 500 ml centrifuge bottle, spin 12,000 x g for 12 min at 4 °C (8,500 rpm Sorvall GS-3 rotor). Decant the supernatant, store pellet at -80 °C overnight or longer if needed.
4. Resuspend the frozen pellet on ice in 10 ml Lyse/Wash buffer (50 mM NaH<sub>2</sub>PO<sub>4</sub>, 300 mM NaCl, 10 mM imidazole, pH 8.0) supplemented with 400  $\mu$ l 25% Triton X-100, 100  $\mu$ l 100 mg/ml lysozyme, 50  $\mu$ l 200 mM phenylmethylsulfonyl fluoride (PMSF). Transfer the resuspended pellet to 50 ml Oak Ridge tube.
5. Sonicate lysate 5 times for 30 sec on ice with 30 sec intervals. Spin sonicated lysate in oak ridge tube at 39,000 x g for 20 min at 4 °C (18,000 rpm Sorvall SS-34 rotor).
6. While the lysate is spinning, wash 1 ml Ni-NTA agarose with 10 ml Lyse/Wash buffer and spin at 1,200 rpm for 5 min at 4 °C. (all further washes/elutions use centrifugation under these conditions). Aspirate wash.

7. Add bacterial supernatant from Step 1.5 to Ni-NTA agarose, shake gently for 2.5 hr at 4 °C. Spin to collect supernatant. Combine 30 µl of supernatant with 10 µl 4x SDS sample buffer and save for purity analysis. Wash the beads 4 times in Lyse/Wash buffer and once in Tris/salt buffer (50 mM Tris, 300 mM NaCl, pH 8.0).
8. Elute 3 times by adding 1 ml Elution buffer (250 mM imidazole in Tris/salt buffer) and 5 µl 1 M dithiothreitol (DTT) to beads, incubating on ice for 10 min, spinning and collecting the supernatant. SLO is a very redox-sensitive protein, and must be kept on ice at all times. Once reduced, the protein will rapidly lose its activity if warmed to 37 °C, even for a short period of time.
9. Wash 500 µl polymyxin-conjugated agarose in elution buffer, spin at 10,000 x g for 1 min at 4 °C and resuspend in 500 µl. To deplete endotoxin, add 200 µl beads to each elution and shake 4 °C for 30 min. Spin at 10,000 x g for 1 min at 4 °C, and save the supernatant. Combine 30 µl of each elution with 10 µl 4x SDS sample buffer for SDS-PAGE analysis.
10. Test the purity of elutions by SDS-PAGE. Boil samples saved for gel analysis at 95 °C for 5 min and load 10 µl on a 10% gel. Stain gel with Coomassie to visualize protein (**Figure 2A**). SLO is 69 kDa. Perform a Bradford Assay to determine protein concentration (typical yield is 4 mg/ml for first two elutions, but may vary by bacterial strain and plasmid used).
11. Test the hemolytic activity of each elution (see below). Pool elutions where purity, concentration and hemolytic activity are satisfactory. Aliquot SLO in single-use aliquots (typically 5-10 µl), freeze on dry ice and store at -80 °C.

## 2. Hemolytic Assay

1. Wash sheep red blood cells (RBCs) in RBC Assay buffer (0.3% bovine serum albumin (BSA), 2 mM CaCl<sub>2</sub>, 10 mM Hepes, pH 7.4), spin at 1,200 rpm for 5 min, and resuspend at 2.5% RBCs in 10 ml RBC Assay buffer.
2. Add 10 µl RBC assay buffer/well in 96-well V-bottom plate on ice. Serially dilute each elution in duplicate. Typical dilution ranges are 1:1,000 to 1:512,000. Include 3 wells with no toxin and 3 wells with 10 µl 2% Triton X-100 as minimum and maximum wells, respectively.
3. Cover plate and incubate at 37 °C 30 min. Centrifuge at 1,200 rpm for 5 min. Transfer 70 µl of supernatant to a flat bottom 96 well plate. Read A<sub>405</sub>. One unit is the dilution of toxin required for 50% lysis of the RBCs. Toxin activity is 1 unit\* dilution factor/0.01 ml.

## 3. Cell Lytic Assay

1. Harvest cells, count, spin. Resuspend at 2x10<sup>6</sup>/ml in buffer R/B (RPMI with 2 mM CaCl<sub>2</sub>, 0.5% BSA) and 20 µg/ml propidium iodide. Add 100 µl cells to a 96-well V-bottom plate.
2. Serially dilute SLO to 2x final concentration in buffer R/B, add 100 µl toxin or 100 µl buffer R/B to cells. Incubate 5 min 37 °C. Typical final concentrations range from 2,000 U/ml to 31.25 U/ml.
3. Run cells on flow cytometer and collect data with filters for phycoerythrin (PE). A one-log shift represents transiently permeabilized cells while a 3 log shift indicates dead cells<sup>4</sup>. Calculate the specific lysis of the cells by subtracting the percentage of dead cells in the control (%PI<sup>high</sup><sub>ctl</sub>) from the experimental (%PI<sup>high</sup><sub>exp</sub>), as follows: specific lysis = (%PI<sup>high</sup><sub>exp</sub> - %PI<sup>high</sup><sub>ctl</sub>) / (100 - %PI<sup>high</sup><sub>ctl</sub>) \* 100

## 4. Micropipette Delivery of Toxin to Cells in Culture Dishes

1. One day prior to experiment, plate 2x10<sup>5</sup> macrophages on a collagen-coated glass-bottom 35 mm dish.
2. Turn on microscope and microinjector. Allow heated stage time to warm to 37 °C. The choice of microscope usually depends on what is locally available. The microscope needs an inverted stage, a stage capable of heating the dishes to 37 °C, excitation/emission filter cubes appropriate for the dye chosen, and the space to physically connect the microinjector. A Bertrand lens is helpful for microinjection, but not required. The computer driving the microscope needs sufficient memory to collect and store data.
3. Label cells for 30 min with dye at 37 °C. Depending on the assay, labeling may be done with 5 µl Fura2 AM in 1 ml PBS or 2 µl calcein AM in 1 ml full media. For Fura2, excitation/emission is collected for 340/510 nm and 380/510 nm, and the ratio of 340/380 signals determines calcium flux. For calcein, excitation/emission is 495/515 nm while ethidium homodimer is 525/620 nm and APC is 650/660 nm. Other labels may be chosen as well.
4. Wash cells with PBS and place in 1 ml RPMI supplemented with 2 mM CaCl<sub>2</sub>. Mount on microscope.
5. Dilute toxin and dextran in water, and centrifuge at 20,000 x g 10 min for 4 °C. Typically, 1 µl SLO and 4 µl 10 mg/ml dextran-555 is diluted in 6 µl water. Dextran or another fluorescent fluid-phase molecule is used to verify that the femto-tip is not clogged, and injects as desired.
6. Load femto-tip from rear with 0.07 µl of diluted toxin using a microloader.
7. Load femto-tip onto microinjector. Adjust angle of injector so that the tip will sit over the center of the cells with room to move in all directions. Clear z-limit. Injection settings should be injecting for 0.5 sec at 120 psi with 20 psi back pressure. Lower tip until it enters the medium.
8. Using the Bertrand lens, center the tip and follow the tip as it is lowered closer to the cells. Once you lose focus, switch back to normal optics. The needle shadow should be apparent in the field. Focus above the cells and lower the needle until it is in focus. Focus back on the cells and carefully bring the needle adjacent to a cell. Set the z-limit for injection. Commence imaging, move tip to desired position, inject to release toxin at the desired time point. Raise the needle, move to a new region of cells and inject. Move needle to home position to prevent any undesired toxin leakage from the needle.

## Representative Results

Typically 10<sup>7</sup>-10<sup>8</sup> U/ml SLO can be obtained with a protein concentration of 4 mg/ml. The amount of toxin required for cell lysis varies by cell type, but is usually 125-500 U/ml SLO (**Figure 2B**). Cell types like macrophages can be more resistant (4000 U/ml) though others (especially T cell lines) are more sensitive. These sensitivities correspond with commercially available SLO. Toxin activity decreases roughly 2-fold with each freeze-thaw, so hemolytic assays with each batch or thaw of toxin are needed to verify toxin activity. Toxin is also very sensitive to heat and oxidation<sup>10</sup> in the absence of cholesterol-containing membranes, so care must be taken when working with the protein.

Microdelivery of the toxin allows the comparison of untreated cells with toxin-treated cells in the same dish. It also provides an internal control to toxin activity, since a diffusion gradient will be established from the micropipette tip. Regions close to the micropipette will show cell death,

typified by calcein loss and ethidium homodimer uptake, whereas regions further away from the tip will show no damage (**Figure 3**). Given the potency of the toxin used, small amounts that leak from the micropipette even in the presence of back pressure can destroy cells as the tip is moved along the field (**Figure 3**). Using the safety option on the microinjector will avoid this loss.

Microdelivery of the toxin also allows the examination of real-time events, such as calcium flux (**Figure 4**). This flux cannot be observed in fixed cells, and the localized delivery of the toxin permits the study of how this induced calcium flux is propagated through a cell culture. Care must be taken not to injure the cells with the micropipette itself, as this can also induce calcium flux<sup>11</sup>.

In addition to standard wide-field microscopy, microdelivery can be combined with high speed 3D confocal microscopy. The advantage of a confocal microscope over wide field is the ability to resolve events in the z-dimension and analyze individual planes. With current technologies, use of a spinning disc confocal is necessary to achieve the high speeds needed. These advantages allow the visualization of microparticles being shed from dendritic cells following toxin injection (**Figure 5**). These microparticles are shed as part of the cellular repair process<sup>4</sup>. Toxin molecules are concentrated on blebs, which are shed to eliminate toxin<sup>4</sup>. Without confocal imaging, detecting the microparticles would be difficult, and potentially lead to the conclusion that toxin is not eliminated in this manner.

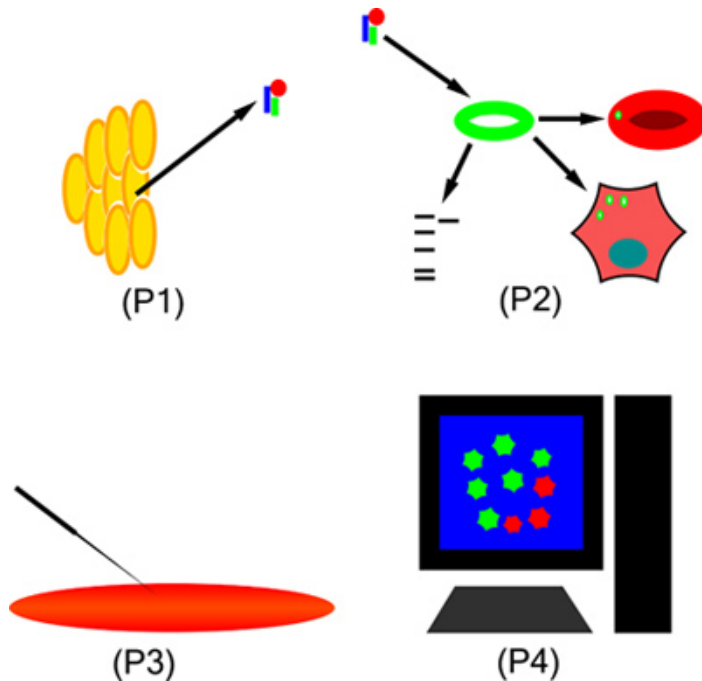


**Figure 1.** Overall workflow for generating and utilizing toxins in live cell imaging. Toxin is purified, subjected to rigorous quality control, and then delivered via micropipette to cells that have been previously labeled with viability dyes, calcium indicators or antibodies to surface proteins. Data is acquired on the microscope and then analyzed using software, such as Metamorph or Elements.

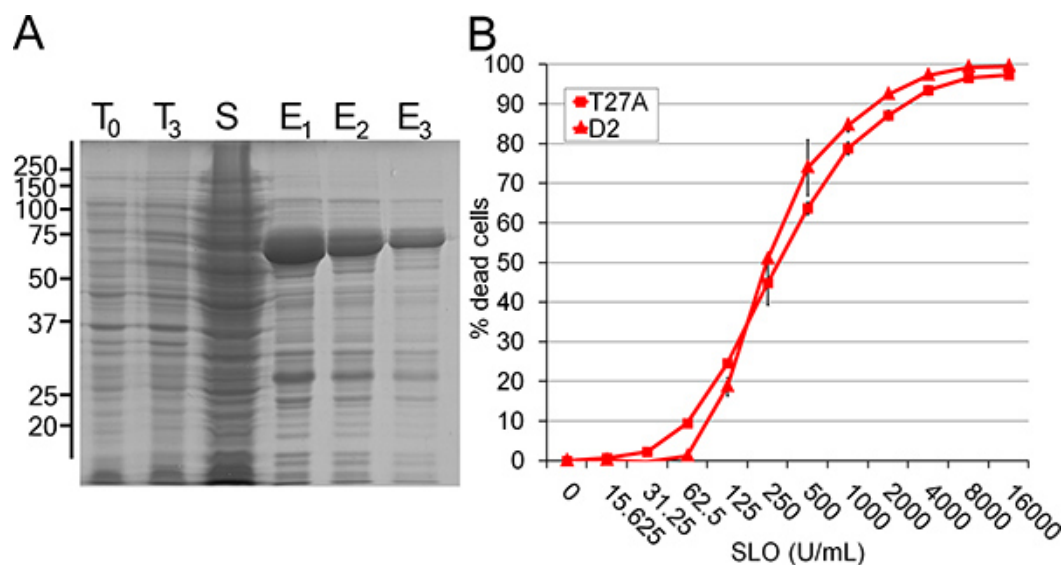


**Figure 2.** Quality control of purified SLO. (A) Samples of bacteria before (T<sub>0</sub>) and after (T<sub>3</sub>) toxin induction, supernatant following purification (S), and each of three elutions (E<sub>1</sub>-E<sub>3</sub>) were resolved by SDS-PAGE and stained with Coomassie blue. (B) Either dendritic cell line D2 or leukemia cell line T27A were challenged with various concentrations of SLO for 5 min at 37 °C in the presence of propidium iodide and examined by flow cytometry. The specific lysis was determined by the following formula:  $\text{specific lysis} = (\%PI^{\text{high}}_{\text{exp}} - \%PI^{\text{high}}_{\text{ctl}}) / (100 - \%PI^{\text{high}}_{\text{ctl}}) * 100$

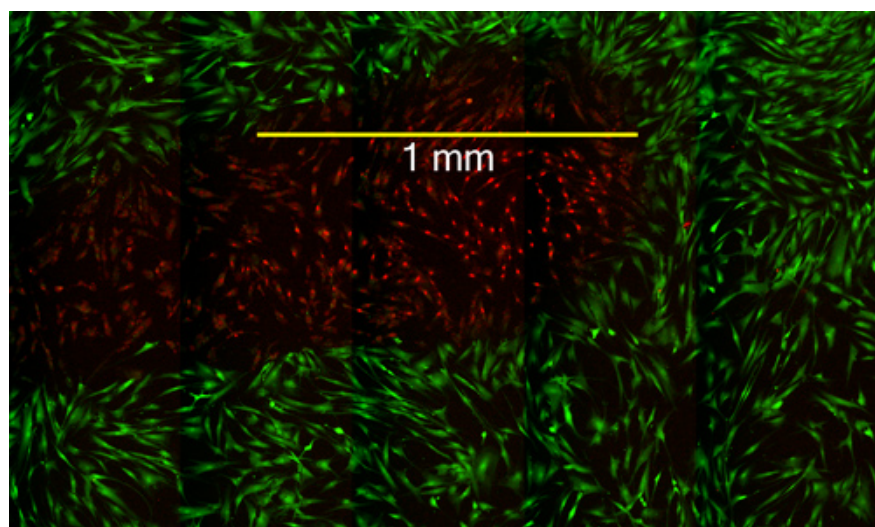


**Figure 3.** Cell death shown by loss of calcein signal and uptake of EtBr in human dermal fibroblasts following localized exposure to the bacterial toxin anthrolysin O. Fibroblasts were incubated with calcein AM and ethidium homodimer using a live dead kit from Life Technologies. 100 pg of the cholesterol binding toxin anthrolysin O<sup>13</sup> (a gift from Dr. Richard Rest, Drexel University) was delivered by micropipette into the center of the culture dish, and widefield fluorescence images collected using a 40x objective after 30 min. Images from multiple fields were combined to generate the larger image shown using Metamorph.



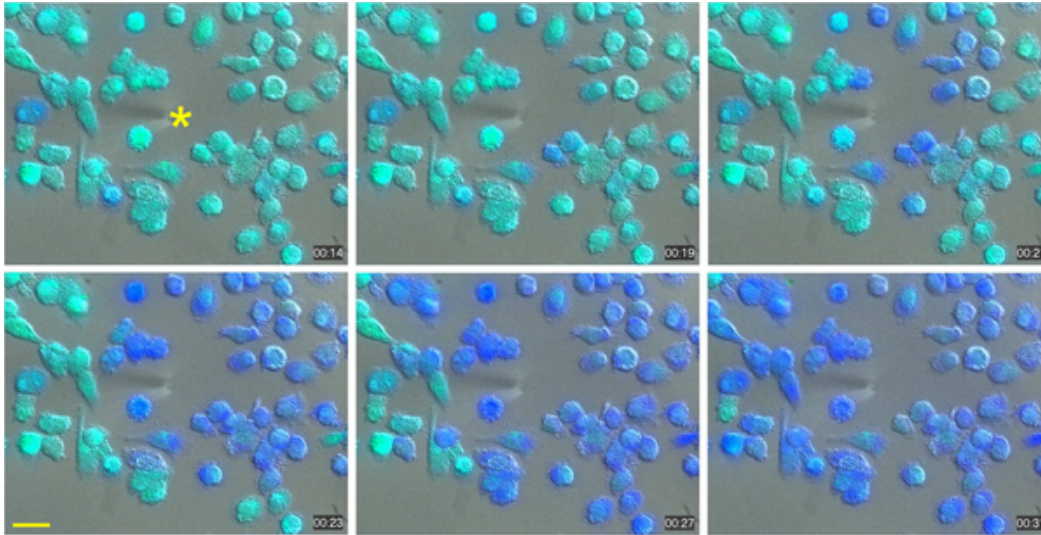


**Figure 4.** Calcium influx into cytosol of human dendritic cells exposed to the bacterial toxin SLO. Cells were loaded with fura2 AM before delivery of a solution of SLO at a concentration of 80 U/ $\mu$ l and a flow rate of 1 nl/min. The tip of the micropipette used for delivery is indicated at time 0 by a yellow asterisk. Images were collected continuously in widefield mode at 340 and 380 nm excitation wavelengths, and the ratio of emissions used to determine cytosolic calcium levels. Shift from green to blue pseudocolor indicates an increase in cytosolic calcium levels. The time mark in each panel indicates seconds after beginning addition of toxin. Scale bar is 20  $\mu$ m. [Click here to view larger figure.](#)

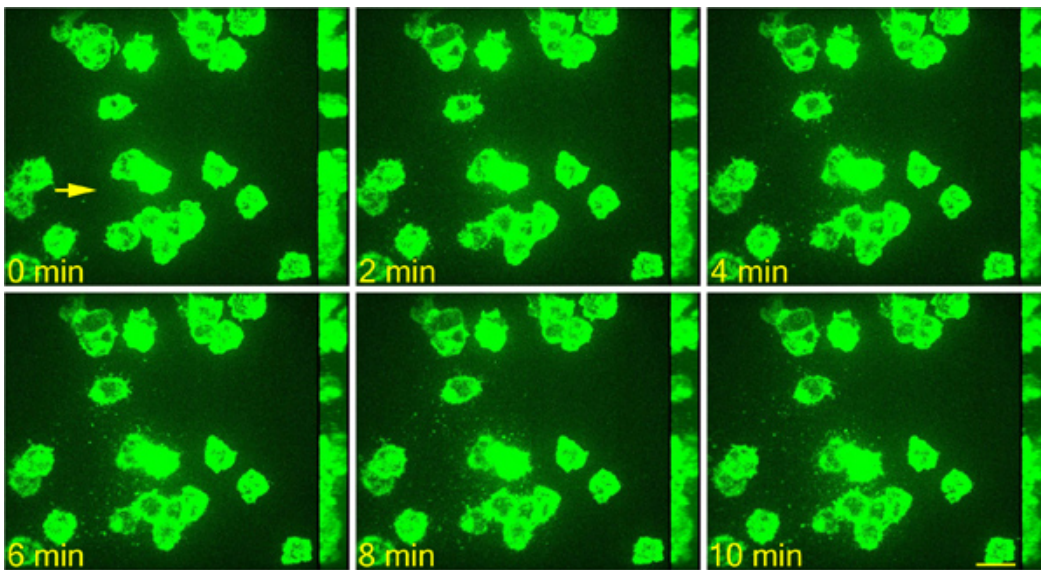


**Figure 5.** Release of microvesicles from the surface of dendritic cells exposed to SLO. Cells were pre-incubated with anti-CD11c conjugated to APC to label the plasma membrane, followed by delivery of a bolus of  $3 \times 10^{-3}$  U of SLO. 3-D reconstructions were generated from confocal z-stacks collected at each time point indicated in minutes. The tip of the microinjector was identified using DIC imaging and is indicated by the yellow arrow. Scale bar is 20  $\mu$ m.

## Discussion

The techniques described here allow the examination of the responses of immune cells to bacterial toxins. The most critical step is the handling and dosing of the toxin. Toxin activity can be extremely variable, even between different aliquots of the same preparation, due to its fragility. This necessitates either testing each aliquot of toxin against a reference cell line or RBCs or using toxin gradients. Toxin gradients, as delivered by micropipette, allow the full spectrum of toxin-induced activities to be observed in real-time, but does not lend itself to biochemical analysis.

Micropipette delivery of the toxin can be challenging. Unlike standard microinjection, however, penetration of the cell is not required for this assay. In fact, care must be taken not to damage the cells with the needle itself, as this will elicit a similar membrane repair response<sup>12</sup>. In immune cells, particularly, the calcium fluxes generated by needle contact will propagate via nanotubes to other cells within the culture<sup>11</sup>. Not injecting cells will also extend the lifetime of the needle. Similarly, use of a Bertrand lens to follow the needle's descent to the cells removes some uncertainty in the positioning of the micropipette. Although damaged needles will leak toxin more rapidly than intact needles, they may still be used to generate preliminary results. The microinjector system allows for multiple injections, should a higher toxin gradient be desired. Alternatively, injection duration can also be modified to alter the dose delivered. The microinjector also allows multiple experiments to be

performed within one dish. Furthermore, the effect of rechallenge can be studied. Although we describe experiments examining immune cells, these methods could be adapted to other cell lines as well.

## Disclosures

No conflicts of interest declared.

## Acknowledgements

The authors would like to thank Richard Rest for the generous gift of anthrolysin O, Michael Caparon for the generous gift of the SLO plasmid and Jonathon Franks for technical assistance. This work was funded by NIH grants T32CA82084 (PAK), and R01AI072083 (RDS).

## References

1. Walev, I., *et al.* Delivery of proteins into living cells by reversible membrane permeabilization with streptolysin-O. *Proc. Natl. Acad. Sci. U.S.A.* **98**, 3185-3190, [pii] 051429498 doi:10.1073/pnas.051429498 (2001).
2. Walev, I., *et al.* Potassium regulates IL-1 beta processing via calcium-independent phospholipase A2. *J. Immunol.* **164**, 5120-5124, [pii] ji\_v164n10p5120 (2000).
3. Scolding, N.J., *et al.* Vesicular removal by oligodendrocytes of membrane attack complexes formed by activated complement. *Nature.* **339**, 620-622, doi:10.1038/339620a0 (1989).
4. Keyel, P.A., *et al.* Streptolysin O clearance through sequestration into blebs that bud passively from the plasma membrane. *J. Cell. Sci.* **124**, 2414-2423, [pii] jcs.076182 doi:10.1242/jcs.076182 (2011).
5. MacKenzie, A., *et al.* Rapid secretion of interleukin-1beta by microvesicle shedding. *Immunity.* **15**, 825-835, [pii] S1074-7613(01)00229-1 (2001).
6. Qu, Y., Franchi, L., Nunez, G., & Dubyak, G.R. Nonclassical IL-1 beta secretion stimulated by P2X7 receptors is dependent on inflammasome activation and correlated with exosome release in murine macrophages. *J. Immunol.* **179**, 1913-1925, [pii] 179/3/1913 (2007).
7. Andrei, C., *et al.* Phospholipases C and A2 control lysosome-mediated IL-1 beta secretion: Implications for inflammatory processes. *Proc. Natl. Acad. Sci. U.S.A.* **101**, 9745-9750, [pii] 0308558101 doi:10.1073/pnas.0308558101 (2004).
8. Franchi, L., Eigenbrod, T., Munoz-Planillo, R., & Nunez, G. The inflammasome: a caspase-1-activation platform that regulates immune responses and disease pathogenesis. *Nat. Immunol.* **10**, 241-247, [pii] ni.1703 doi:10.1038/ni.1703 (2009).
9. Magassa, N., Chandrasekaran, S., & Caparon, M.G. Streptococcus pyogenes cytolysin-mediated translocation does not require pore formation by streptolysin O. *EMBO Rep.* **11**, 400-405, [pii] embor201037 doi:10.1038/embor.2010.37 (2010).
10. Pinkney, M., Beachey, E., & Kehoe, M. The thiol-activated toxin streptolysin O does not require a thiol group for cytolytic activity. *Infect. Immun.* **57**, 2553-2558 (1989).
11. Watkins, S.C. & Salter, R.D. Functional connectivity between immune cells mediated by tunneling nanotubes. *Immunity.* **23**, 309-318, [pii] S1074-7613(05)00269-4 doi:10.1016/j.immuni.2005.08.009 (2005).
12. McNeil, P.L., Vogel, S.S., Miyake, K., & Terasaki, M. Patching plasma membrane disruptions with cytoplasmic membrane. *J. Cell. Sci.* **113** (Pt. 11), 1891-1902 (2000).
13. Shannon, J.G., Ross, C.L., Koehler, T.M., & Rest, R.F. Characterization of anthrolysin O, the Bacillus anthracis cholesterol-dependent cytolysin. *Infect. Immun.* **71**, 3183-3189 (2003).